7ICMSNSE-45

Assessment of the No-Core Melt Concept for the Canadian SCWR Conceptual Design

C. Azih¹

¹ Canadian Nuclear Laboratories, Chalk River, Ontario, Canada chuk.azih@cnl.ca

Abstract

To meet the safety goals outlined by the Generation IV International Forum, the conceptual design of the Canadian Super-Critical Water-cooled Reactor (SCWR) constrains the peak temperature of the fuel cladding below its melting temperature following a loss of coolant accident (LOCA) with loss of emergency core cooling (LOECC). Transient simulations performed using a thermoelastic model coupled with CATHENA (Canadian Algorithm for THErmalhydraulic Network Analysis) analyses indicate that during LOCA/LOECC the fuel and fuel channel components will remain some margin below their respective melting points. Potential design options exist to further decrease the peak temperatures of the fuel channel components during LOCA/LOECC.

Keywords: Generation IV Reactors, Fuel and Fuel Channels, CATHENA Analyses

1. Introduction

Canada is presently developing a pressure-tube type Super-Critical Water-cooled Reactor (SCWR) to meet the safety, economic, sustainability, and proliferation resistance targets set by the Generation IV International Forum (GIF) [1]. To meet the enhanced safety requirements outlined by the GIF, the fuel channel design for the Canadian SCWR constrains the peak temperature of the fuel sheath/cladding below its melting temperature (~1300°C) following a loss of coolant accident (LOCA) with loss of emergency core cooling (LOECC). This constraint, termed no-core melt, aims to reduce or eliminate fission product release under such postulated accident scenarios, thereby reducing the negative consequences of such accidents. The insulated pressure tube concept, termed High Efficiency Channel (HEC), was identified as a viable concept for mitigating the consequences of a LOCA/LOECC. A schematic of the fuel and fuel channel concept for the Canadian SCWR is shown in Figure 1. The pressure tube is thermally isolated from the primary coolant by an encapsulated insulator to ensure that the pressure tube outer surface temperature is maintained below the saturation temperature of the moderator fluid during normal operation. The insulator is clad with an inner and outer liner tube to ensure that it maintains its integrity during its service life. To minimize the peak temperature of the fuel cladding during a postulated LOCA/LOECC scenario, sufficient decay heat must be transferred from the fuel to the moderator. However, to enhance the thermal efficiency of the power cycle during normal operation, radial heat loss from the fuel/coolant to the moderator should be minimized. Thus, the HEC geometry should optimized to both reduce radial heat loss across the fuel channel during normal operation and increase the radial heat loss during LOCA/LOECC accident scenarios.

Using CATHENA (Canadian Algorithm for THErmalhydraulic Network Analysis) thermalhydraulics code, simulations for evaluating the thermal performance of the HEC concept have been previously performed for the 43-element fuel bundle designs [2], for a 54-element bundle design [3], and for a 78-element fuel bundle design [4]. In light of significant changes to the fuel and fuel channel design for the Canadian SCWR, the no-core melt analysis for the HEC is revisited in the present work. Also,

some simplifying assumptions made in the previous analyses are reassessed in the present work to reflect the more advanced stage of the Canadian SCWR design.

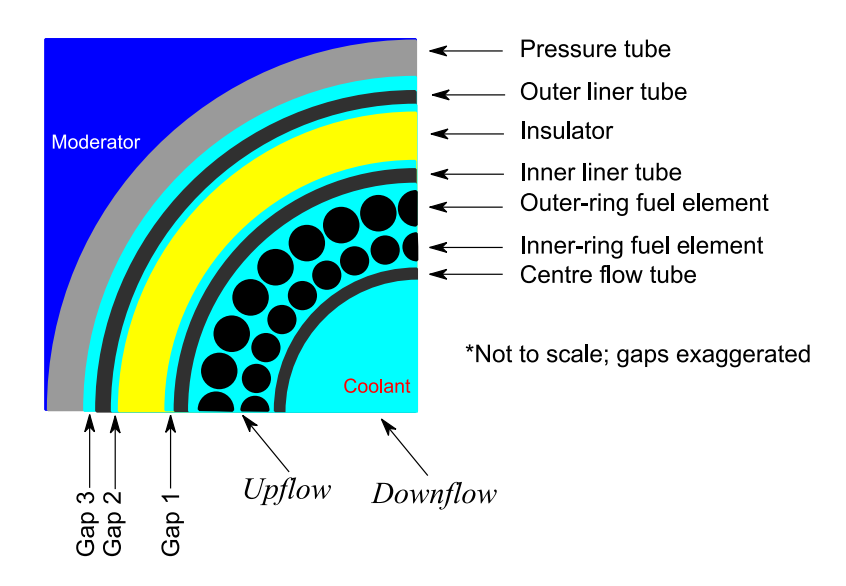


Figure 1 Cross-section of the fuel channel for the Canadian SCWR

2. Modelling of Fuel and Fuel Channel Behaviour

2.1 Fuel and Fuel Channel Components

The Canadian SCWR conceptual design proposes a 64-element fuel bundle concept consisting of two rings of fuel elements as illustrated in Figure 1. The relevant dimensions for the fuel and fuel channel components used in the present analysis are presented in Table 1.

2.2 Model Theories

To satisfy the no-core melt concept decay heat must be removed from the fuel and transferred to the moderator, which may be cooled through a passive moderator cooling system (PMCS) during LOCA/LOECC. Sufficient decay heat must be removed to assure that the fuel sheath does not melt and the pressure boundary is not compromised. However, it is also of interest to minimize radial heat loss from the fuel and coolant to the moderator during normal operation. These requirements are achieved by the opening/closing of anticipated radial gaps between the fuel channel components. Thus it is of interest to model the heat transfer behaviour of all components and the thermoelastic/plastic behaviour of the liner tubes, insulator and pressure tube at both normal and accident conditions. CATHENA [5] is coupled with thermoelastic computations to model these behaviours at both normal and accident conditions. The thermoelastic computations are summarized in Section 2.2.2.

Table 1 Fuel and Fuel Channel Constituents and Geometry

Component	Material	ID (mm)	OD (mm)
Pressure tube	Zr-2.5Nb	157.0	181.0
Outer liner**	310 Stainless Steel (310 SS)	156.0	157.0
Insulator**	Yttria-Stabilized zirconia (YSZ)	145.0	156.0
Inner liner**	310 SS	144.0	145.0
Centre flow tube	310 SS	92.0	94.0
Fuel pellet (inner ring)	15 wt% PuO ₂ /ThO ₂	0.0	8.3
Fuel pellet (outer ring)	12 wt% PuO ₂ /ThO ₂	0.0	8.8
Fuel sheath (inner ring)	310 SS	8.3	9.5
Fuel sheath (outer ring)	310 SS	8.8	10.0

^{**} Geometry of the liner tubes and insulator are not fixed. These components will be optimized through the no-core melt analysis.

2.2.1 CATHENA Model Theory

The modelling theory for CATHENA is documented in [5]; the present analysis uses CATHENA-Mod3.5d Rev. 3.

2.2.2 Thermoelastic Model Theory

The change in the radius of a component can be obtained from the hoop (i.e., diametral) strain through the following relation:

$$r_{new} = r_{old} \left(1 + \varepsilon_{\theta} \right) \tag{1}$$

Where ε is the strain, r is the radius and the subscript θ represents the circumferential coordinate. In the present assessment, it is assumed that all thermal deformation occurs in the elastic mode. For the plane-strain approximation, which is valid for geometries where the length dimension is much greater than the cross-sectional dimensions, the hoop strain is given by [6]:

$$\varepsilon_{\theta} = \frac{(1+\nu)}{F} [(1-\nu)\sigma_{\theta} - \nu\sigma_{r}] + \alpha (1-\nu)(T - T_{ref})$$
(2)

where σ is the normal stress, E is the modulus of elasticity, v is Poisson's ratio, α is the coefficient of thermal expansion, T is the temperature, T_{ref} is a temperature at which component is not deformed thermally, and the subscript r indicates the radial direction. The total normal stresses are a summation of the mechanical and thermal stresses. The mechanical stresses are defined as [6]:

7th International Conference on Modelling and Simulation in Nuclear Science and Engineering (7ICMSNSE) Ottawa Marriott Hotel, Ottawa, Ontario, Canada, October 18-21, 2015

$$\sigma_{r,M} = \frac{P_i r_i^2 - P_o r_o^2 + \frac{r_i^2 r_o^2}{r^2} (P_i - P_o)}{r_o^2 - r_i^2}$$
(3)

$$\sigma_{\theta,M} = \frac{P_i r_i^2 - P_o r_o^2 + \frac{r_i^2 r_o^2}{r^2} (P_o - P_i)}{r_o^2 - r_i^2}$$
(4)

where, P is the pressure, the subscripts i and o indicate the internal and external/outside surface of the cylinder, respectively. The thermal components of stress are given by [7]:

$$\sigma_{r,T} = \frac{E\alpha(T_i - T_o)}{2(1 - \nu)\ln(r_o/r_i)} \left[\ln\left(\frac{r_o}{r}\right) + \frac{r_i^2}{r_o^2 - r_i^2} \left(1 - \frac{r_o^2}{r_i^2}\right) \ln\left(\frac{r_o}{r_i}\right) \right]$$
(5)

$$\sigma_{\theta,T} = \frac{E\alpha(T_i - T_o)}{2(1 - \nu)\ln(r_o/r_i)} \left[1 - \ln\left(\frac{r_o}{r}\right) - \frac{r_i^2}{r_o^2 - r_i^2} \left(1 + \frac{r_o^2}{r_i^2}\right) \ln\left(\frac{r_o}{r_i}\right) \right]$$
(6)

To calculate the deformation of the components through Equations 1 to 6, the distribution of temperature within each material must be calculated. This is obtained through heat transfer calculations with the following equation:

$$Q = \frac{2\pi Lk(T_1 - T_2)}{\ln(r_2/r_1)} + \frac{\sigma_{SB} 2\pi r_1 L(T_1^4 - T_2^4)}{1/e_1 + r_1/r_2 (1/e_2 - 1)}$$
(7)

where L is the axial length, σ_{SB} is the Stefan-Boltzmann constant, e is the emissivity, k is the thermal conductivity of the medium through which the heat is transferred, and the subscripts 1 and 2 indicate consecutive computational nodes. The radiation heat transfer term in Equation 7 is only calculated at the boundaries between voided components or components filled with gas. Equation 8 is used to calculate the heat transfer at the boundaries for surfaces in contact:

$$Q = h_a A (T_1 - T_2) \tag{8}$$

where h_c is the contact conductance, and A is the heat-transfer-surface area. When the components are in contact, the expression for the contact conductance by Mikic is used [8]:

$$h_c = 1.9(k'/Ra')(p_{if}/E')^{0.94}$$
 (9)

Here, *Ra* is the surface roughness, the subscript *itf* refers to values at the solid-solid interface, and the 'superscript refers to an effective value for both surfaces.

Equations 1 to 9 are implemented in MATLAB Version 6 Release 12.

2.3 Model Verification and Validation

Details of the verification and validation of the CATHENA model are documented by Hanna [5]. The thermoelastic model was verified by comparing simulations with this model to results obtained from ANSYS Mechanical 13.0 using identical geometries and boundary conditions. Validation of the thermoelastic model written in MATLAB programming language was accomplished by simulating the

small-scale low-pressure HEC tests (SSLP tests) preformed by Licht and Cusick [9]. The SSLP tests were performed with a test section that was approximately ½ of the radial scale of the Canadian SCWR fuel channel concept. The test apparatus consisted of an inner liner that was directly heated through joule heating, and a pressure tube that was cooled by flowing water on the outer surface. Tests were performed with several insulator tubes placed between the pressure tube and the liner tube. In this validation exercise, only the tests with non-porous YSZ insulator tubes were simulated (SSLP-14 SSLP-19, SSLP-21). The results of the validation exercise are shown in Figure 2 by plotting the measured and predicted liner tube temperatures for each power set point. The thermoelastic model is observed to perform favourably, and conservatively predicts the liner tube temperatures above 600°C.

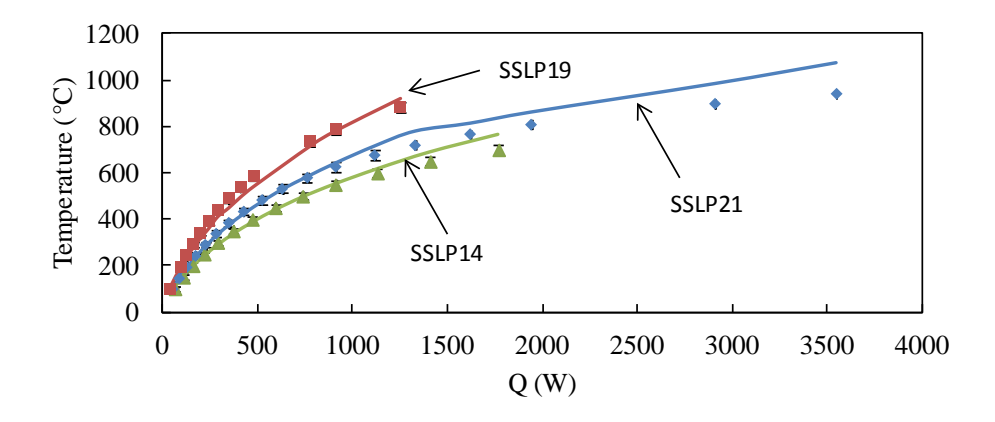


Figure 2 Comparison of liner tube temperatures from thermoelastic model with experimental data from SSLP tests [9]

2.4 Model Approach

The approach for the no-core melt assessment was to use CATHENA to determine an equivalent concentric cylindrical geometry (simple geometry) that represents the thermal radiation heat transfer from the fuel bundle. Then, the simplified geometry in MATLAB was used to determine the effective gap conductance values for the fuel channel as a function of liner tube temperature. Finally, CATHENA was used to model the Canadian SCWR fuel channel behaviour under LOCA/LOECC with the MATLAB-supplied gap conductance look-up tables.

2.4.1 Material Properties

Data from Tye and Salmon [10] and Clark and Tye [11] were used for the temperature-dependent material properties for 310 stainless steel (SS). The surface emissivity for 310 SS was taken as 0.8, which is typical for an oxidized metallic surface. Data from Schlichting et al. [12], Raghavan et al. [13], Gadag and Subbaryan [14], Biswas et al. [15] were used for the temperature-dependent material properties of Yttria-stabilized zirconia (YSZ). Data from Peletsky [16], and Whitmarsh [17] were used to approximate the properties of Zr-2.5 Nb. Material properties for the thorium-plutonium mixed-oxide fuels were obtained using the data of Cozzo et al. [18]. The NIST standard reference database [19] was used to obtain the properties of light water and heavy water for the thermoelastic model and the default properties for light water and heavy water built into CATHENA are used in the CATHENA model [5].

2.4.2 Boundary Conditions for the Thermoelastic Calculations

The primary purpose of the thermoelastic model was to provide gap conductance tables that can be used in CATHENA to account for the effect of radial deformation of the fuel channel components on heat transfer. The geometry for the thermoelastic model consisted of five concentric cylinders, namely:

equivalent cylinder; inner liner tube; insulator; outer liner tube; and pressure tube. These components were modelled with 5 radial nodes. The surface roughness was taken as 1 μ m for all components. To represent normal operating conditions, the surface temperature of the pressure tube was specified as 120°C. To simulate LOCA/LOECC, the outer surface temperature of the pressure tube was specified as 160°C, which is approximately the limit below which nucleate boiling is assured. To obtain gap conductance values from the temperature distribution of each component the following equation is applied:

$$Q = h_{\sigma} A(\Delta T) \tag{10}$$

where h_g is the gap conductance between the boundaries of two solid components, A is the area of the smaller diameter surface, and ΔT is the temperature difference between the boundaries between the two components. The value of h_g represents the contact conductance between two solid components when the components are in contact; otherwise, it represents the effective conductance of the solid components surfaces and fluid between the components, which includes both radiation and conduction heat transfer modes.

2.4.3 Boundary Conditions for the CATHENA Simulations

A single-channel model was used and consisted of the centre flow tube, inner ring fuel, outer ring fuel, inner ring fuel sheath, outer ring fuel sheath, inner liner tube, insulator, outer liner tube, and pressure These components were modelled with ten axial nodes, five radial nodes, and two circumferential nodes except for the fuel pellets which had two circumferential nodes. A simulation was run in which circumferential and radial node distributions were doubled to confirm that the results are not sensitive to the choice of node distribution. To establish steady-state conditions representing normal operation, the flow within the centre flow tube, and the inner liner/centre flow tube annulus were modelled as vertical pipe components having 10 axial nodes with light water 25 MPa as the fluid medium. The moderator was modelled as a vertical pipe component having 10 axial nodes with heavy water at 0.3 MPa and 50°C as the fluid medium. The flowrate of light water was specified such that the temperature of the coolant increased from an inlet value of ~350°C to an outlet value of ~625°C based on the thermal power of the channel. The thermal power values used ranged from 9906 kW to 7559 kW coresponding to the highest power and average power channels, respectively [20]. An axial power peaking factor of 1.19 was used. Heat transferred to the coolant and moderator was calculated using the Dittus-Boelter correlation [21] for the light water flow, and the CATHENA default correlations for the heavy water flow [5].

For the transient LOCA/LOECC calculations, the flow within the centre flow tube, and the inner liner/centre flow tube annulus were modelled as vertical pipe components having 10 axial nodes with stagnant light water at atmospheric pressure and 650°C as the fluid medium. The moderator was modelled as a vertical pipe component having 10 axial nodes with heavy water at 0.3 MPa and 50°C as the fluid medium. The temperatures of the fuel channel components were initialized from the results of the normal operating condition simulations. The decay heat profile in Figure 3 was implemented. Heat transfer to the moderator was calculated using the McAdams correlation [22]. For conservatism, the fuel channel was assumed to be completely voided at accident initiation (0 s) such that heat transfer between the fuel and inner liner tube, and heat transfer within the centre flow tube occurred solely through the radiation mode.

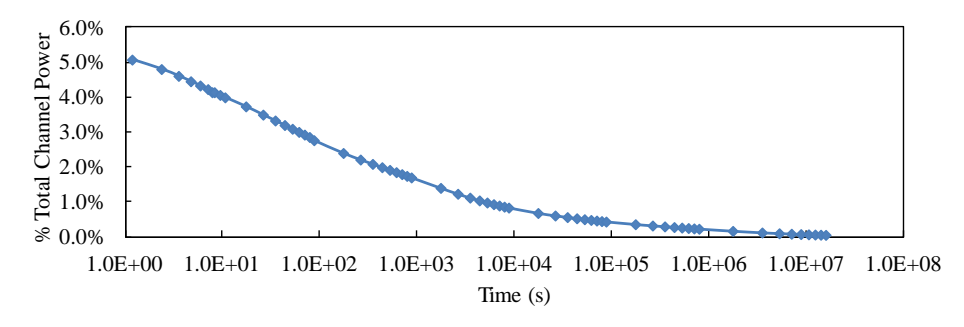


Figure 3 Decay heat profile for no-core melt assessment

3. Results and Discussion

3.1 Effect of Shrink Cladding and Segmentation of Insulator on Fuel Sheath Temperature

Although the primary purpose of the thermoelastic model was to provide gap conductance tables that can be used in CATHENA, it was convenient to perform parts of the no-core melt assessment using the thermoelastic model. The effect of shrink-cladding and segmentation of the insulator were assessed using the thermoelastic model. Under long term cooling following a LOCA/LOECC, each of the gaps in the voided fuel channel depends on radiation heat transfer to remove the heat generated by the fuel. The temperature difference required for radiation heat transfer is typically large and could yield very large overall temperature differences from the fuel sheath to the moderator. Analyses show that if Gaps 1 or 2¹ did not close, the fuel sheath temperature could be as high as ~1600°C which is well beyond its melting temperature of ~1300°C. In these analyses the power is fixed at a decay heat value of 3% of the peak channel power under normal operation (9906 kW). This value is chosen to be conservatively higher than the decay heat power value that is expected when the fuel sheath attains its peak temperature under LOCA/LOECC conditions [4].

An observation from the SSLP test series was that some insulator tubes cracked under stresses induced by the thermal expansion of the liner tube [9], and may therefore not maintain geometrical integrity under LOCA/LOECC conditions. These issues were alleviated by shrink encapsulating the insulator such that Gaps 1 and 2 in Figure 1 were minimized so that the heat transfer behaviour of the fuel channel during normal operation and LOCA/LOECC conditions depends largely on the size of the pressure-tube/outer-liner gap (Gap 3). To achieve a fuel sheath temperature of 1300°C with a constant decay heat of 3% (279 kW), the required pressure-tube/outer-liner gap sizes for circumferentially segmented and non-segmented insulators are compared in Figure 4. It is observed that for equivalent fuel sheath temperatures, a segmented insulator allows for a bigger initial gap between the pressure tube and outer liner tube. This is because the segmented insulator does not provide any resistance to the radial expansion of the liner tube. Based on these analyses, the gap conductance tables for further no-core melt analyses were generated for a shrink-encapsulated circumferentially segmented insulator configuration.

Gap 1 – insulator/inner-liner gap; Gap 2 – outer-liner/insulator gap; Gap 3 – pressure-tube/outer-liner gap

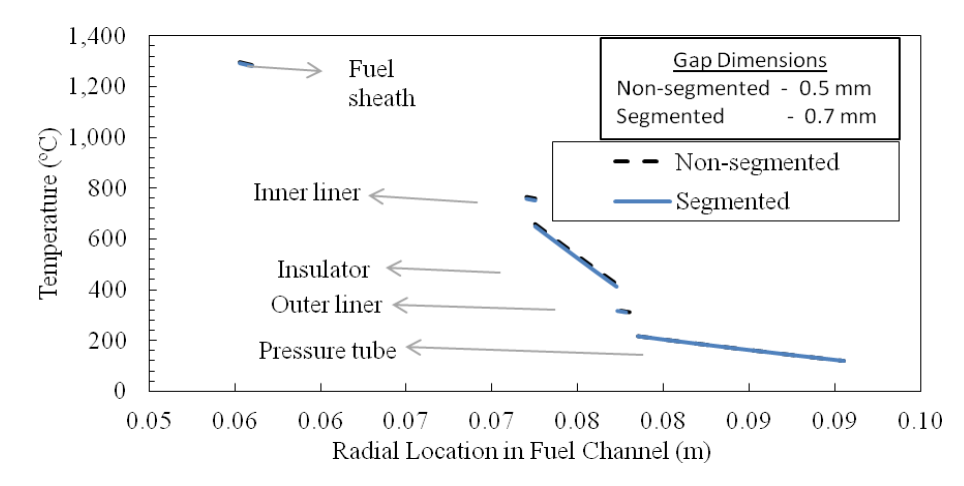


Figure 4 Comparison of radial temperature profile through the fuel channel for circumferentially segmented and non-segmented insulators

3.2 Gap Conductances for HEC Conceptual Design

The thermoelastic model was used to generate gap conductance tables that are indexed by the liner tube temperature. These tables can be used in CATHENA to account for the thermoelastic behaviour of the fuel channel. As discussed in Section 3.1, for a shrink-encapsulated circumferentially segmented insulator configuration only the pressure-tube/outer-liner gap significantly affects the fuel channel heat transfer². The effective gap conductance, calculated by solving for h_g in Equation 10, are plotted for pressure-tube/outer-liner gap values of 0.5, 0.75, 1.0, 1.5, and 2.0 mm in Figure 5. As expected, the gap conductance is observed to increase with increasing gap size.

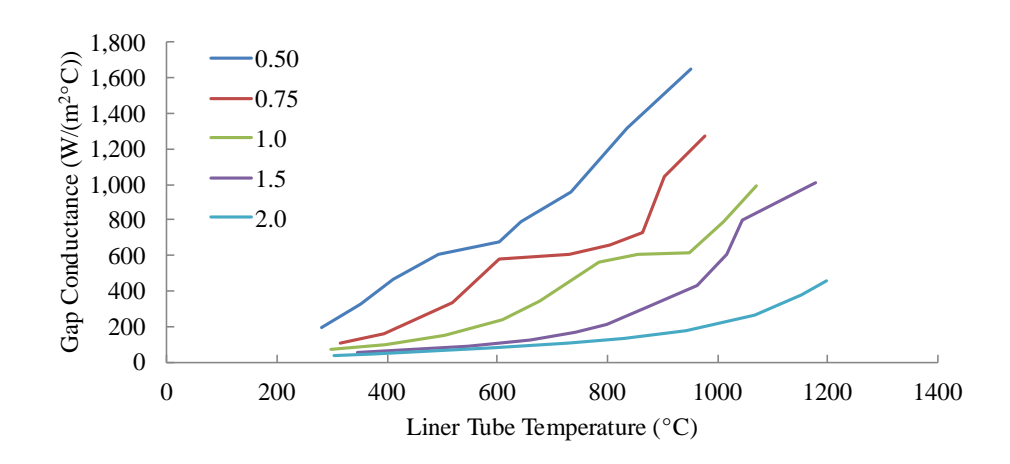


Figure 5 Effective gap conductance for pressure-tube/outler-liner gap

3.3 Assessment of No-Core Melt for the Conceptual Canadian SCWR Design using CATHENA

For the no-core melt assessment in the present study a reference pressure-tube/outer-liner gap design value of 0.75 mm was chosen. The results for this simulation are shown in Figure 6 and Figure 7 for normal operation and accident conditions, respectively. For normal operating conditions, the outer-ring fuel centreline temperature is observed to be ~200°C higher than that of the inner ring, and reaches

² Pressure-tube/outer-liner gap referred to as "gap" in the remainder of the paper where not explicitly denoted.

temperatures just over 2000°C. The fuel sheath temperatures reach values of up to 800°C, while the inner liner and central flow tube maintain a temperature slightly below that of the primary coolant which is ~625°C at the outlet. Across the insulator, the temperature is reduced by ~300°C, allowing the pressure tube to operate in a low temperature environment. Under LOCA/LOECC conditions, the maximum fuel sheath temperature occurs on the inner ring fuel elements. In Figure 7 the temperatures of the fuel and fuel channel components following a LOCA/LOECC are shown for a pressure-tube/outer-liner gap value of 0.75 mm, at the time when the maximum fuel sheath temperature of 1214°C occurred. This peak temperature occurs approximately 2 minutes after initiation of LOCA/LOECC. The peak inner-ring fuel centreline temperature is observed to be ~100°C higher than that of the outer ring. The fuel sheath temperatures are ~30°C lower than their respective fuel temperatures. The centre flow tube temperature is similar to that of the inner-ring fuel sheath. The fuel sheaths radiate heat to the inner liner tube which has a temperature of ~700°C and there is ~250°C temperature drop across the insulator. The pressure tube outer surface temperature remains below 150°C.

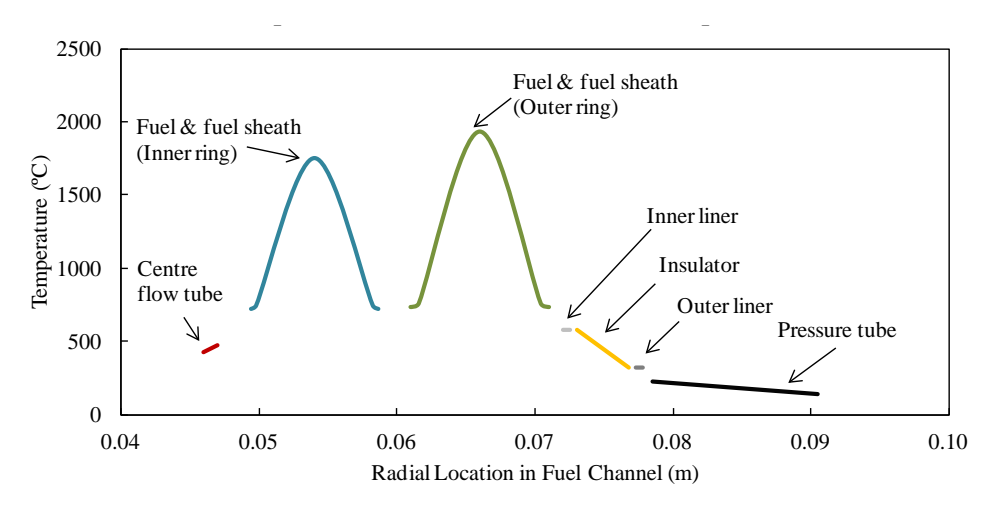


Figure 6 Temperature distribution of fuel and fuel channel during normal operation for 0.75 mm gap between pressure tube and outer liner

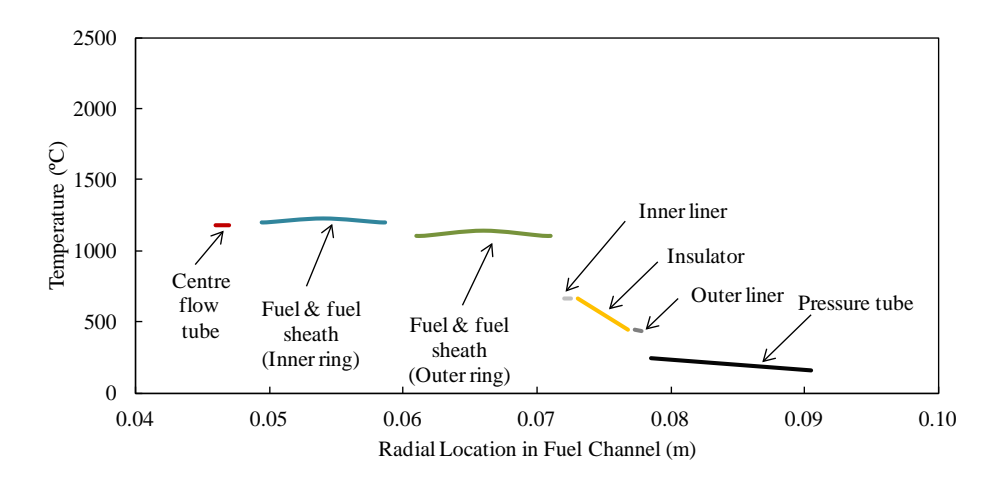


Figure 7 Temperature distribution of fuel and fuel channel during LOCA/LOECC for 0.75 mm gap between pressure tube and outer liner

Figure 8 plots the maximum fuel sheath temperature for LOCA/LOECC at various channel power values as a function of pressure-tube/outer-liner gap sizes. The effect of pressure-tube/outer-liner gap

size is observed in the individual curves in Figure 8, which indicate that as the gap size increases the maximum fuel sheath temperature increases. The maximum fuel sheath temperature occurs approximately two minutes (120 s) after the LOCA/LOECC event occurs. Initially, the monotonicallydecreasing decay heat and the stored energy in the fuel go into elevating the temperature of the fuel channel components. At this stage, there is minimal heat being transferred to the moderator. When the temperature of the components of the fuel channel are sufficiently high, the gap between the outer liner tube and the pressure tube closes to an extent that notable amounts of heat can be transferred to the moderator. The heat transferred to the moderator is a combination of the decay heat generated by the fuel and the stored energy in the fuel and fuel channel components. Eventually, heat transfer to the moderator is higher than heat storage by the fuel and fuel channel components, yielding a slow decrease in the temperatures of these components. It is expected that as the initial gap size increases, the maximum fuel sheath temperature will also increase. When the gap is larger the fuel channel components will be in the heat storage phase for a longer period since it will take longer for a larger gap to close. Accordingly, the maximum fuel sheath temperature occurs at ~120 s for the 0.75 mm gap; whereas, for the 2.0 mm gap, the maximum fuel sheath temperature occurs at ~250 s. For the full range of gaps sizes studied, the maximum fuel sheath temperature remains lower than 1300°C, which is below the melting point of 310 stainless steel. A notable increase in maximum sheath temperature with gap size appears to occur for gaps greater than 1 mm and the sensitivity of the maximum sheath temperature to the initial gap size appears to increase with decreasing channel power.

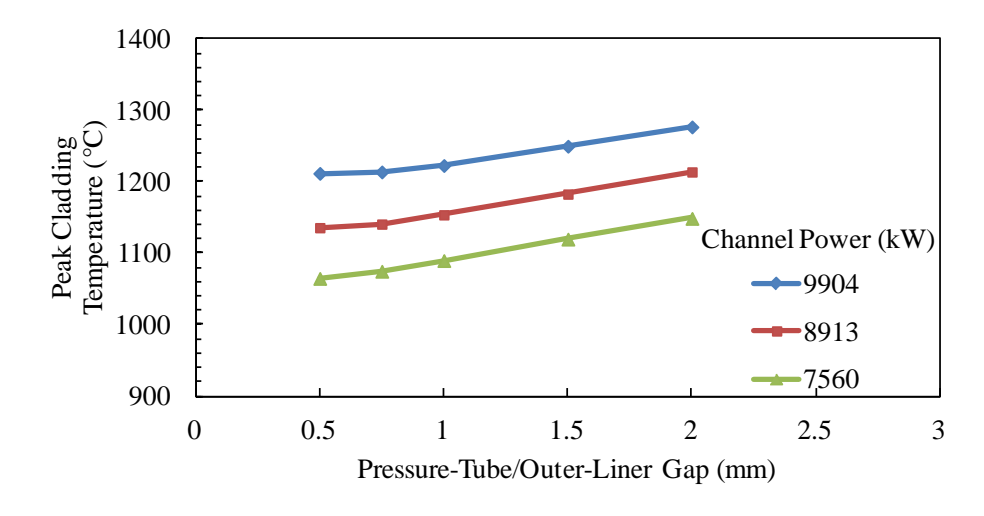


Figure 8 Maximum fuel sheath temperature for various channel powers and pressuretube/outer-liner gap sizes under LOCA/LOECC

4. Summary

The HEC fuel channel design for the Canadian SCWR has the potential to support the improved safety requirement, outlined by the GIF, by ensuring that the fuel and fuel channel components maintain their integrity following a postulated LOCA/LOECC scenario. The no-core melt assessment of the Canadian SCWR was performed by using a thermoelastic model with simplified channel geometry to generate gap conductance tables for the fuel channel to implement in CATHENA for modelling the behaviour of the fuel channel under long term cooling following a LOCA/LOECC. The results show that the maximum fuel sheath temperature can potentially be maintained below its melting temperature under long term cooling following a LOCA/LOECC. The peak fuel sheath temperature was observed to occur approximately two minutes after LOCA/LOECC.

5. References

- [1] L. Leung, M. Yetisir, W. Diamond, D. Martin, J. Pencer, B. Hyland, H. Hamilton, D. Guzonas and R. Duffey, "A next generation heavy water nuclear reactor with supercritical water as coolant", <u>The International Conference on Future of Heavy Water Reactors (HWR-Future)</u>, Ottawa, ON, Canada, 2011 October 2-5
- [2] A. Vasic and H. Khartabil, "Passive Cooling of the CANDU SCWR fuel at LOCA/LOECC Conditions", Proceedings of GLOBAL 2005, Tsukuba, Japan, 2005 October 9-13
- [3] J. Shan, Y. Jiang and L. Leung, "Subchannel and Radiation Heat Transfer Analysis of 54-Element CANDU-SCWR Bundle", <u>Proc. 5th Int'l Sym. on Supercritical Water-Cooled Reactors</u>, Vancouver, BC, Canada, 2011 March 13-16
- [4] J. Licht and R. Xu, "Preliminary No-Core Melt Assessment for the High Efficiency Channel Preconceptual Design", <u>The 3rd China-Canada Joint Workshop on Supercritical-Water-Cooled Reactors</u>, 2012 April 18-20
- [5] B.N. Hanna, "CATHENA: A thermalhydraulic code for CANDU analysis", Nuclear Engineering and Design, Vol. 180, No. 2, 1998, pp. 113-131
- [6] P.P. Benham, R.J. Crawford and C.G. Armstrong, "Mechanics of Solid Materials", Longman Group Ltd., 1996
- [7] R.B. Hetnarski and M. Resa Eslami, "Thermal Stresses Advanced Theory and Applications", Springer, 2009
- [8] B. Mikic, "Thermal contact conductance; theoretical considerations", Internal Journal of Heat and Mass Transfer, Vol. 17, No. 2, 1974, pp. 205-214
- [9] J. Licht and L. Cusick, "Progress on the Insulated Fuel Channel Experiments for the Canadian Supercritical Water Reactor", <u>The 3rd China-Canada Joint Workshop on Supercritical-Water-Cooled Reactors</u>, 2012 April 18-20
- [10] R.P. Tye and D.R. Salmon, "Development of new thermal conductivity reference materials: A summary of recent contributions by national physical laboratory", In Thermal conductivity standards 27/Thermal expansion, 15th Ed. E. Porter, 2005
- [11] J. Clark and R. Tye, "Thermophysical properties reference data for some key engineering alloys", High Temperatures-High Pressures, Vol. 35/36 No. 1, 2003, pp. 1-14
- [12] K.W. Schlichting, N.P. Padture and P.G. Klemens, "Thermal conductivity of dense and porous yttria-stabilized zirconia", Journal of Material Science, Vol. 36, No. 12, 2001, pp. 3003-3010
- [13] S. Raghavan, H. Wang, W.D. Porter, R.B. Dinwiddie and M.J. Mayo, "Thermal properties of zirconia co-doped with trivalent and pentavalent oxides, Acta Mater", Vol. 49, 2001, pp. 169-179
- [14] S. Gadag and G. Subbaryan, "Thermoelastic properties of dense YSZ and porous Ni-ZrO₂ monolithic and isotropic materials", Journal of Material Science, Vol. 41, 2006
- [15] M. Biswas, C.S. Kumbhar and D.S. Gowtam, "Characterization of Nanocrystalline Yttria-Stabilized Zirconia: An In Situ HTXRD Study", ISRN Nanotechnology, 2011
- [16] V.E. Peletsky, "High-temperature thermal conductivity of zirconium based alloys", High Temperatures-High pressures, Vol. 31, 1999, pp. 627-632
- [17] C.L. Whitmarsh, "Review of Zircaloy-2 and Zircaloy-4 Properties Relevant to N.S. Savannah Reactor Design", Oak Ridge National Laboratory: ORNL-3281, TID-5400, 17th Ed., 1962

- [18] C. Cozzo, D. Staicu, J. Somers, A. Fernandes and R.S. Konings, "Thermal diffusivity and conductivity of thorium-plutonium mixed oxides", Journal of Nuclear Materials, Vol. 416, 2011, pp. 135-141
- [19] E.W. Lemmon, M.O. McLinden and D.G. Friend, "Thermophysical Properties of Fluid Systems in NIST Chemistry WebBook", NIST Standard Reference Database Number 69, Eds. P.J. Linstrom and W.G. Mallard, National Institute of Standards and Technology, Gaithersburg MD, 20899, http://webbook.nist.gov, (retrieved 2014 January)
- [20] M.H. McDonald et al., "Pre-Conceptual Fuel Design Concepts for the Canadian SuperCritical Water-Cooled Reactor", The 5th Int'l Sym. on Supercritical Water-Cooled Reactors (ISSCWR-5), Vancouver, BC, Canada, 2011 March 13-16
- [21] R.H.S. Winterton, "Where did the Dittus and Boelter equation come from?", International Journal of Heat and Mass Transfer, Vol. 41, No. 4-5, 1998, pp. 809-810
- [22] W.H. McAdams, "Heat Transmission", 3rd Ed., McGraw-Hill, 1954